Initial Design of a W-band Superconducting Kinetic Inductance Qubit

Farzad B. Faramarzi [*1,2], Peter K. Day[†3], Jacob Glasby [‡1,5], Sasha Sypkens [§2], Marco Colangelo [¶7], Ralph Chamberlin [‖1], Mohammad Mirhosseini [**6], Kevin Schmidt [††1], Karl K. Berggren [‡‡7], and Philip Mauskopf [§§1,2]

[1]Department of Physics, Arizona State University, USA
[2]School of Earth and Space Exploration, Arizona State University, USA
[3]Jet Propulsion Laboratory, NASA, USA
[5]School of Electrical, Computer, and Energy Engineering, Arizona State University, USA
[6]Department of Electrical Engineering, California Institute of Technology, USA
[7]Department of Electrical Engineering and Computer Science, Massachusetts Institute of Technology,USA

March 16, 2021

Abstract

Superconducting qubits are widely used in quantum computing research and industry. We describe a superconducting kinetic inductance qubit (and introduce the term Kineticon to describe it) operating at W-band frequencies with a nonlinear nanowire section that provides the anharmonicity required for two distinct quantum energy states. Operating the qubits at higher frequencies may relax the dilution refrigerator temperature requirements for these devices and paves the path for multiplexing a large number of qubits. Millimeter-wave operation requires superconductors with relatively high T_c, which implies high gap frequency, $2\Delta/h$, beyond which photons break Cooper pairs. For example, NbTiN with $T_c = 15\,\mathrm{K}$ has a gap frequency near 1.4 THz, which is much higher than that of aluminum (90 GHz), allowing for operation throughout the millimeter-wave band. Here we describe a design and simulation of a W-band Kineticon qubit embedded in a 3-D cavity. We perform classical electromagnetic calculations of the resulting field distributions.

[*]ffarama1@asu.edu
[†]peter.k.day@jpl.nasa.gov
[‡]jglasby@asu.edu
[§]ssypkens@asu.edu
[¶]colang@mit.edu
[‖]ralph.chamberlin@asu.edu
[**]mohmir@caltech.edu
[††]kevin.schmidt@asu.edu
[‡‡]berggren@mit.edu
[§§]Philip.Mauskopf@asu.edu

Superconducting qubits are one of the leading platforms for building quantum computers. Recently, quantum supremacy, in which a quantum computer performs a computation which is infeasible on a classical computer, was demonstrated using 53 superconducting qubits [1]. Several companies and academic institutions (IBM, Rigetti, QuTech, and Amazon) offer cloud quantum computing services based on superconducting transmon qubits. These devices, op-

erating in the 4-10 GHz band utilize Josephson junctions formed by an aluminum oxide layer between aluminum contacts. Scaling up these early quantum computers to the thousands or millions of physical qubits needed to realize quantum error correction [2] faces several major hurdles including limited coherence (10-100 T_2^* is typical), lack of room temperature interconnects, and the large physical size of superconducting qubits (typical qubits have 0.1-1 mm lateral dimensions). The standard aluminum or niobium Josephson tunnel junction is becoming a bottleneck to increasing qubit coherence and yield requirements: Spurious two level systems (TLS) cause decoherence [3, 4, 5], imprecision in qubit frequencies reduces yield for fixed frequency qubit architectures [6], and quasipartlces cause charge parity fluctuations and heating [7]. Superconducting kinetic inductance qubits operating in the W-band (75-110 GHz) have the potential to lift these bottlenecks. The nonlinear inductance of superconducting nanowires has been used in designs and experiments involving cavity-based parametric amplifiers [8, 9] and qubits [10, 11, 12] in the sub-10 GHz regime and as a parametric amplifier in the W-band [13], but thus far, a viable superconducting qubit has not been demonstrated in the W-band.

In particular, exploration of high-frequency qubits is encouraged because they have the potential to solve current problems with state-of-the-art transmon qubits. In order to achieve the highest coherence times, IBM uses fixed-frequency transmons and an all-microwave operation to entangle pairs of qubits together (the cross resonance gate). However, the speed and performance of the cross resonance gate depends heavily on the exact frequency allocation between the qubits [6] and spectator qubits [14]. Fabricating the nonlinear inductive part of the qubit from well-defined lithographic processes of non-linear kinetic superconductors instead of amorphous growth of an aluminum oxide layer in the Josephson junction could allow repeatable frequency allocation between qubits. Also operating at a higher frequency offers the ability to scale the systems down in size as we look to scale to ever larger numbers of qubits.

Construction of a quantum computer implementing error correction imposes constraints on size, operating frequency, and operating temperature. The computer will require at least thousands of physical qubits, a scale at which the physical size of the circuits residing at milliKelvin temperatures becomes a limitation. This is particularly true for qubits coupled to 3D microwave cavities, but also holds for 2D circuits. An interesting possibility is to scale the circuits to a much higher frequency. Millimeter-wave operation requires superconductors with relatively high T_c, which implies high gap frequency, $2\Delta/h$, beyond which photons break Cooper pairs. For example NbTiN with $T_c \approx 15\,\mathrm{K}$ [15] has a gap frequency near 1.4 THz, much higher than that of aluminum (90 GHz), allowing for operation throughout the millimeter-wave band. We introduce the new term Kineticon to refer to qubits that take advantage of the nonlinear response of superconducting wires as opposed to relying on Josephson junctions.

In this section, we quantize the Kineticon system following closely the standard treatment for quantizing electrical circuits[16, 17].

A Kineticon qubit is very similar to an LC resonator circuit, save for the inductive part of the circuit, which is non-linear. A simple Kineticon qubit circuit can be imagined as in Fig 1, with one active node and no current bias. Defining a branch flux at this node, the kinetic inductance of the nanowire in the weak anharmonic limit, $\Phi \approx L_{0k} I$ can be written as [18]

$$L_k(\Phi) \approx L_{0k}\left(1 + \frac{\Phi^2}{\Phi_*^2}\right) \tag{1}$$

where L_{0k} is the kinetic inductance with zero bias and $\Phi_* \equiv I_* L_{0k}$ where I_* is a characteristic current parameter of the nonlinearity.

The energy stored in the capacitor and the nonlinear inductor can be found using

$$E(t) = \int_{-\infty}^{t} v_b(t') i_b(t') dt' \tag{2}$$

where v_b and i_b are the voltage and current of the branch, respectively[16]. Calculated energies are as

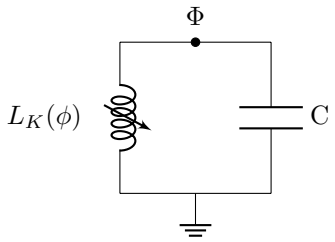

Figure 1: Circuit diagram of an ideal superconducting LC resonator with nonlinear inductive element.

follows

$$U_C = \frac{1}{2}C\dot{\Phi}^2 \tag{3}$$

$$U_L \approx E_k\left(\frac{\Phi^2}{\Phi_*^2} - \frac{\Phi^4}{\Phi_*^4}\right) \tag{4}$$

where we define $E_k = \frac{\Phi_*^2}{2L_{0k}}$. The Lagrangian is given by

$$\mathcal{L} = U_C - U_L = \frac{1}{2}C\dot{\Phi}^2 - E_k\left(\frac{\Phi^2}{\Phi_*^2} - \frac{\Phi^4}{\Phi_*^4}\right). \tag{5}$$

Now using Legendre transformation $\mathcal{H} = \dot{\Phi}Q - \mathcal{L}$ we can write the Hamiltonian as follows

$$\mathcal{H} = \frac{Q^2}{2C} + E_k\left(\frac{\Phi^2}{\Phi_*^2} - \frac{\Phi^4}{\Phi_*^4}\right). \tag{6}$$

We can quantize the circuit by replacing Q and Φ with their quantum operators that satisfy the following commutation relation

$$[Q, \Phi] = -i\hbar. \tag{7}$$

The Hamiltonian operator now can be written as follows by replacing charge and flux with their quantum operators

$$\tilde{H} = \frac{\tilde{Q}^2}{2C} + \frac{\tilde{\Phi}^2}{2L_{0k}} - \frac{1}{2L_{0k}\Phi_*^2}\tilde{\Phi}^4. \tag{8}$$

In the second quantization language, we can define the following creation and annihilation operators

$$\tilde{a} = \frac{1}{\sqrt{\hbar\omega_r}}\left[\frac{1}{\sqrt{2L_{0k}}}\tilde{\Phi} + i\frac{1}{\sqrt{2C}}\tilde{Q}\right] \tag{9}$$

$$\tilde{a}^\dagger = \frac{1}{\sqrt{\hbar\omega_r}}\left[\frac{1}{\sqrt{2L_{0k}}}\tilde{\Phi} - i\frac{1}{\sqrt{2C}}\tilde{Q}\right]. \tag{10}$$

The reduced charge and flux operators in terms of $\tilde{a}$ and $\tilde{a}^\dagger$ are given by

$$\tilde{q} = \frac{\tilde{Q}}{q_{zpf}} = i\left(\tilde{a} - \tilde{a}^\dagger\right) \tag{11}$$

$$\tilde{\phi} = \frac{\tilde{\Phi}}{\varphi_{zpf}} = \left(\tilde{a} + \tilde{a}^\dagger\right). \tag{12}$$

where $Z_0 = \sqrt{\frac{L_{0k}}{C}}$ and we defined $\varphi_{zpf} = \sqrt{\frac{\hbar Z_0}{2}}$ and $q_{zpf} = \sqrt{\frac{\hbar}{2Z_0}}$ as zero-point fluctuations of flux and charge respectively.

The Hamiltonian of our weakly anharmonic oscillator (AHO) becomes

$$\tilde{H} = \hbar\omega_r\left[a^\dagger a + \frac{1}{2} + \frac{1}{4}\lambda\left(a^\dagger + a\right)^4\right] \tag{13}$$

where $\omega_r = \sqrt{\frac{1}{L_{0k}C}}$ and $\lambda = -\frac{\varphi_{zpf}^2}{\Phi_*^2}$.

Addressing individual states in a qubit requires a large relative anharmonicity, $\alpha = |E_{10} - E_{21}|/E_{10}$, where E_{10} is the transition energy from the ground state to the first-excited state and E_{21} is the transition energy from first-excited state to the second-excited state. Here, we derive this expression for the Kineticon qubit, and discuss the implications of this requirement.

Increasing both the qubit and readout resonator frequency to W-band ($\sim$ 100 GHz) could allow for operation of the quantum processor at a higher temperature. While the 90 GHz gap frequency of aluminum represents a barrier for conventional qubit technologies, it may be possible to realize a qubit with a transition frequency in the millimeter band that uses nonlinear kinetic inductance to provide the required anharmonicity. For a Kineticon qubit the

relative anharmonicity, α can be written as follows

$$\alpha \approx 3\frac{I_{zpf}^2}{I_*^2} \tag{14}$$

where $I_{zpf} = \sqrt{\frac{hf_r}{2L}}$ is the zero-point fluctuation current and I_* is the characteristic current of the nanowire. The factor 3 comes from energy eigenvalue calculations for a nanowire in the weak anharmonic limit. For a Kineticon qubit with $f_r = 100$ GHz, we can plot the relative anharmonicity as functions of total inductance of the nanowire L and the characteristic current I_*. As we can see from Fig.2, lowering both total inductance L and the characteristic current I_* increases the relative anharmonicity. To improve the anharmonicity of a Kineticon qubit, it is possible to control J_* and L_s of the nanowire during the fabrication process [19, 20] in addition to changing its dimensions.

We can express I_* of the nanowire in terms of the material parameters using Mattis-Bardeen Theory[21] and following [22] as

$$I_* = J_* wt = \sqrt{\frac{\pi N(0)\Delta^3}{\hbar\rho_n}} wt \tag{15}$$

where w and t are the width and thickness of the nanowire respectively and ρ_n is the normal state resistivity of the thin film. Using $L_s = \hbar R_s/\pi\Delta$, we can express the relative anharmonicity in terms of the volume, V, of the nanowire:

$$\alpha \approx 3\frac{hf_r}{2N(0)\Delta^2 V}, \tag{16}$$

where f_r is the resonator frequency, $N(0)$ is the density of states at the Fermi level, and Δ is the gap parameter. Here we assume the resonator inductance is dominated by that of the nanowire. The denominator in this expression is the superconducting condensation energy, which may also be expressed in terms of the critical field. Using $N(0) = 8.7 \times 10^9 \text{eV}^{-1}\mu\text{m}^{-3}$[23] and $\Delta = 0.5$meV for a thin TiN film ($T_c = 4.5$ K and gap frequency of $f_{gap} \approx 265$ GHz), $N(0) = 2\times10^{10}$ eV $^{-1}\mu\text{m}^{-3}$ and $\Delta = 1.1$ meV [24, 25] for a NbN thin film, and setting a nanowire thickness to 5 nm and the length and width to be equal, the anharmonicity is shown in Fig. 2.

While an absolute anharmonicity comparable to a transmon ($\sim$ 200 MHz) may be achieved with dimensions that are more or less straightforward to produce, the question is whether TLS or other loss mechanisms will contribute a loss tangent of ($\sim 10^{-6}$) for this type of qubit, as they do for current state-of-the-art microwave qubits. In that case, to maintain the ratio of decay time to read time the anharmonicity would need to be increased accordingly, requiring increased length or decreased width, so the fabrication becomes more challenging. We need to investigate non-linearity in resonators with embedded nanowires in order to better understand the design requirements.

Apart from the possibility of high frequency operation, an advantage of circuits made from relatively high T_c materials is that they can be less affected by quasiparticles:

- The thermal quasiparticle density goes as $e^{-2\Delta/T}$.
- The mean number of non-thermal quasiparticles produced by absorption of a phonon of a given energy is $\xi h\nu/\Delta$, where ν is the phonon frequency and ξ is a material dependent parameter (around 0.5 for most materials).
- Quasiparticles that are created through leakage of radiation into the cryogenic environment recombine at a rate that scales as T_c^{-3} [26].

In addition to lower quasiparticle loss, the nitride superconductors that we will study may be affected less by loss and decoherence associated with two level systems. It is known, for example, that TiN and NbTiN have high quality surfaces and form more stable and thinner oxide layers [27], unlike elemental superconductors such as Al, Nb and Ta. TiN in particular is a hard material and is used as a coating on machine tools, drill bits, etc. Groups working on kinetic inductance detectors have found that fabricating the non-photoresponsive parts of the detectors out of NbTiN leads to lower TLS

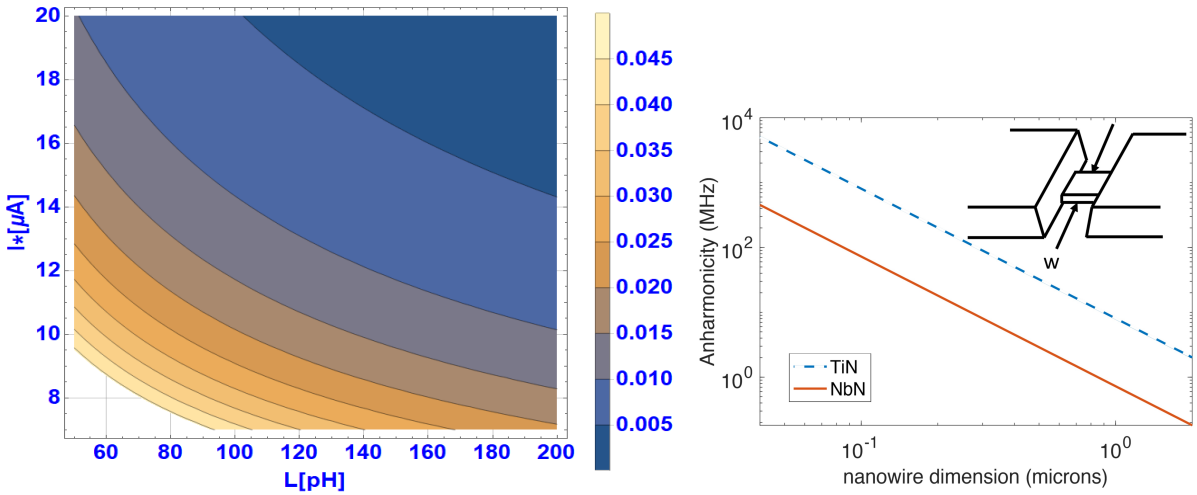

Figure 2: Contour plot of the relative anharmonicity of a nanowire qubit as a function of total inductance L and the characteristic current I_*. Anharmonicity versus nanowire dimension for a 100 GHz resonator with an inductance dominated by an embedded TiN and NbN nanowire. The anharmonicity increases with decreasing nanowire dimensions, and is larger for TiN than NbN.

noise [28, 29]. Recent results on transmon qubits using Ta electrodes have shown an improvement over state-of-the-art coherence times [30], which was associated with the favorable properties of the tantalum oxide surface, so it is interesting to ask whether the metal nitride superconductors, and other potential materials for Kineticons, will provide further improvement.

In this section, we present designs corresponding to two stages of development of the Kineticon qubit. The first design is based on thin film technology and is most appropriate for early-stage investigations while the second design is a more complete three-dimensional design in which the qubit is coupled to a readout cavity and is more appropriate for later-stage work.

To investigate the anharmonicity in different materials and structures, we have designed a nanowire with different dimensions embedded in a thin-film Fabry-Perot resonator. The nanowire is placed in the middle of the resonator where the current has an anti-node at the fundamental frequency f_0 $(\lambda/2)$ as shown in Fig.3. Since the inductance of the resonator is dominated by the kinetic inductance of the nanowire, any change in the kinetic inductance caused by adjusting the readout power shifts the resonant frequency. Putting the nanowire in the above mentioned configuration helps us to measure the frequency shift due to very small number of photons in the resonator. For such a qubit we require the frequency shift δf to be larger than number of photons n times the bandwidth B, $\delta f > nB/2\pi$ [31].

To put a W-band tone into the resonator we designed a single mode rectangular waveguide to CPW transition and capacitively couple the signal to the resonator. We use am commercially available electromagnetic simulator Ansys Electronics Suite (HFSS) [32] to simulate and optimize the coupling efficiency of the transition[33].We expect a coupling efficiency of 70 percent or better at 100 GHz.

Eventually, this technology will require coupling to other qubits, which can be achieved by embedding

the qubit in a three-dimensional cavity. That cavity also could reduce the influence of defects in the thin-film system by increasing the mode volume and reducing the field density [34].

To embed the Kineticon qubit in a 3D resonant readout cavity, we have designed and simulated a 100 GHz resonant cavity coupled to two waveguides through evanescent couplers as shown in Fig.4.a. The dimensions of the cavity was adjusted such that the resonant frequency of the cavity-substrate system is nearly 100 GHz. In this case the dimensions of the cavity are; width = 1 mm, height = 2.54 and depth = 1.4 mm. The Kineticon qubit is placed in the middle of the cavity where the dipole moment of the qubit is aligned with the TE_{101} mode and where the electric field is maximum. The transmission response of the cavity-qubit system is shown in Fig.4.c where both qubit and cavity modes are visible.

In conclusion, we have investigated and simulated the possibility of a W-band qubit resonator by taking advantage of the non-linear kinetic inductance of a nanowire as the anharmonic element. Increasing the operating frequency and readout frequency of the qubits relaxes the very low temperature requirement. Higher frequency also means smaller cavity and qubit dimensions, which helps with scaling up the number of qubits for quantum computation.

The approach we suggest has a number of possible problems with it: (1) the new materials we plan to use might prove to induce new sources of noise and decoherence; (2) the high frequencies we plan to work at may be challenging to synthesize and control in performing qubit operations; and (3) the operation at higher temperatures and frequencies may introduce different kinds of noise and decoherence that have not been previously observed. In addition, our calculations so far have been purely classical—a quantum mechanical treatment is clearly in order. To resolve these questions, additional work will be required.

The first step is to fabricate the Fabry-Perot resonator with the embedded nanowire to measure frequency shifts and estimate the anharmonicity for different materials, such as NbN and TiN, and compare them with the analytical expressions derived in this work. In parallel we plan to fabricate the 3D cavities mentioned here using micro-machining and test them warm and cold. Next step will be to characterize the cavity- qubit system at W-band frequencies.

Acknowledgement

M.C. and K.K.B. acknowledge the support of the National Science Foundation under contract No. ECCS-2000743 (MIT).

References

[1] Arute et. al. Quantum supremacy using a programmable superconducting processor. *Nature*, 574(7779):505–510, October 2019.

[2] Engineering National Academies of Sciences. *Quantum Computing: Progress and Prospects*. December 2018.

[3] P. V. Klimov, J. Kelly, Z. Chen, M. Neeley, A. Megrant, B. Burkett, R. Barends, K. Arya, B. Chiaro, Yu Chen, A. Dunsworth, A. Fowler, B. Foxen, C. Gidney, M . Giustina, R. Graff, T. Huang, E. Jeffrey, Erik Lucero, J. Y. Mutus, O. Naaman, C. Neill, C. Quintana, P. Roushan, A. Sank, Daniel a nd Vainsencher, J. Wenner, T. C. White, S. Boixo, R. Babbush, V. N. Smelyanskiy, H. Neven, and John M. Martinis. Fluctuations of Energy-Relaxation Times in Superconducti ng Qubits. *Physical Review Letters*, 121(9):090502, August 2018.

[4] Jonathan J. Burnett, Andreas Bengtsson, Marco Scigliuzzo, David Niepce, Marina Kudra, Per Delsing, and Jonas Bylander. Decoherence benchmarking of superconducting qubits. *npj Quantum Information*, 5(1):1–8, June 2019. Number: 1 Publisher: Nature Publishing Group.

[5] Steffen Schlör, Jürgen Lisenfeld, Clemens Müller, Alexander Bilmes, Andre Schneider, David P. Pappas, Alexey V. Ustinov, and Martin Weides. Correlating Decoherence in Transmon

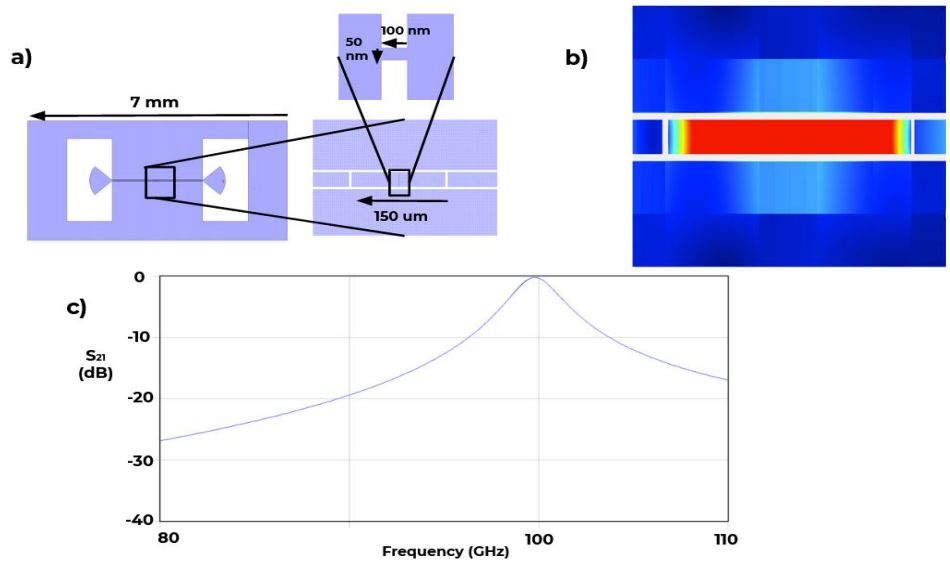

Figure 3: [illegible]

Qubits: Low Frequency Noise by Single Fluctuators. [illegible], 123(19):190502, November 2019. Publisher: American Physical Society.

[6] Christopher Chamberland, Guanyu Zhu, Theodore J. Yoder, Jared B. Hertzberg, and Andrew W. Cross. Topological and Subsystem Codes on Low-Degree Graphs with Flag Qubits. [illegible], 10(1):011022, January 2020. Publisher: American Physical Society.

[7] K. Serniak, M. Hays, G. de Lange, S. Diamond, S. Shankar, L. D. Burkhart, L. Frunzio, M. Houzet, and M. H. Devoret. Hot Nonequilibrium Quasiparticles in Transmon Qubits. [illegible], 121(15):157701, October 2018. Publisher: American Physical Society.

[8] R. Vijay, J. D. Sau, Marvin L. Cohen, and I. Siddiqi. Optimizing anharmonicity in nanoscale weak link josephson junction oscillators. [illegible], 103:087003, Aug 2009.

[9] E. M. Levenson-Falk, R. Vijay, and I. Siddiqi. Nonlinear microwave response of aluminum weak-link josephson oscillators. [illegible], 98(12):123115, 2011.

[10] Patrick Winkel, Kiril Borisov, Lukas Grünhaupt, Dennis Rieger, Martin Spiecker, Francesco Valenti, Alexey V. Ustinov, Wolfgang Wernsdorfer, and Ioan M. Pop. Implementation of a transmon qubit using superconducting granular aluminum. [illegible], 10:031032, Aug 2020.

[11] Yannick Schön, Jan Nicolas Voss, Micha Wildermuth, Andre Schneider, Sebastian T. Skacel, Martin P. Weides, Jared H. Cole, Hannes Rotzinger, and Alexey V. Ustinov. Rabi oscillations in a superconducting nanowire circuit. [illegible], 5(1):1–5, March 2020. Number: 1 Publisher: Nature Publishing Group.

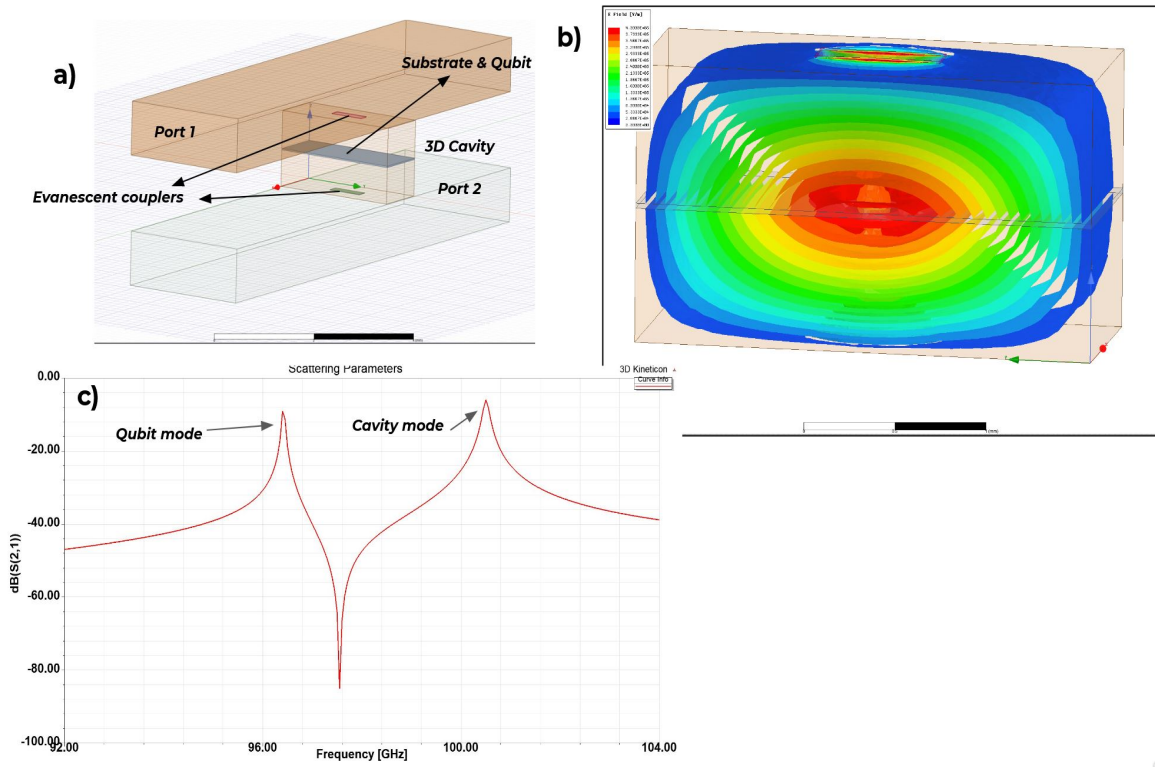

Figure 4: *a) [illegible]*

c) S_{21} calculated [illegible]

[12] Andrew J. Kerman. Metastable superconducting qubit. , 104:027002, Jan 2010.

[13] Alexander Anferov, Aziza Suleymanzade, Andrew Oriani, Jonathan Simon, and David I. Schuster. Millimeter-wave four-wave mixing via kinetic inductance for quantum devices. , 13:024056, Feb 2020.

[14] Maika Takita, A. D. Córcoles, Easwar Magesan, Baleegh Abdo, Markus Brink, Andrew Cross, Jerry M. Chow, and Jay M. Gambetta. Demonstration of weight-four parity measurements in the surface code architecture. , 117:210505, Nov 2016.

[15] R. Basu Thakur, N. Klimovich, P. K. Day, E. Shirokoff, P. Mauskopf, F. Faramarzi, and P. S. Barry. Superconducting on-chip fourier transform spectrometer. , 200:342–352, October 2020.

[16] J Devoret, M. H. Zinn-Justin. Quantum fluctuations in electrical circuits. 1997.

[17] Bernard Yurke and John S. Denker. Quantum network theory. , 29:1419–1437, Mar 1984.

[18] P. D. Mauskopf. Transition edge sensors and kinetic inductance detectors in astronomical instruments. , 130(990):082001, jun 2018.

[19] Thomas Aref and Alexey Bezryadin. Precisein situtuning of the critical current of a superconducting nanowire using high bias voltage pulses. , 22(39):395302, sep 2011.

[20] Anthony J Annunziata, Daniel F Santavicca, Luigi Frunzio, Gianluigi Catelani, Michael J Rooks, Aviad Frydman, and Daniel E Prober. Tunable superconducting nanoinductors. , 21(44):445202, oct 2010.

[21] D. C. Mattis and J. Bardeen. Theory of the anomalous skin effect in normal and superconducting metals. , 111:412–417, Jul 1958.

[22] Jonas Zmuidzinas. Superconducting microresonators: Physics and applications. , 3(1):169–214, 2012.

[23] Henry G Leduc, Bruce Bumble, Peter K Day, Byeong Ho Eom, Jiansong Gao, Sunil Golwala, Benjamin A Mazin, Sean McHugh, Andrew Merrill, David C Moore, et al. Titanium nitride films for ultrasensitive microresonator detectors. , 97(10):102509, 2010.

[24] Edward Schroeder. . PhD thesis, Arizona State University, 2018.

[25] Alexej Semenov, Burghardt Günther, Ute Böttger, H-W Hübers, Holger Bartolf, Andreas Engel, Andreas Schilling, Konstantin Ilin, Michael Siegel, R Schneider, et al. Optical and transport properties of ultrathin nbn films and nanostructures. , 80(5):054510, 2009.

[26] SB Kaplan, CC Chi, DN Langenberg, Jhy-Jiun Chang, S Jafarey, and DJ Scalapino. Quasiparticle and phonon lifetimes in superconductors. , 14(11):4854, 1976.

[27] Lu Zhang, Lixing You, Liliang Ying, Wei Peng, and Zhen Wang. Characterization of surface oxidation layers on ultrathin nbtin films. , 545:1 – 4, 2018.

[28] J. Bueno, O. Yurduseven, S. J. C. Yates, N. Llombart, V. Murugesan, D. J. Thoen, A. M. Baryshev, A. Neto, and J. J. A. Baselmans. Full characterisation of a background limited antenna coupled kid over an octave of bandwidth for thz radiation. , 110(23):233503, 2017.

[29] R. M. J. Janssen, J. J. A. Baselmans, A. Endo, L. Ferrari, S. J. C. Yates, A. M. Baryshev, and T. M. Klapwijk. Performance of hybrid

NbTiN-Al microwave kinetic inductance detectors as direct detectors for sub-millimeter astronomy. In Wayne S. Holland and Jonas Zmuidzinas, editors, *Millimeter, Submillimeter, and Far-Infrared Detectors and Instrumentation for Astronomy VII*, volume 9153, pages 261 – 267. International Society for Optics and Photonics, SPIE, 2014.

[30] Alex PM Place, Lila VH Rodgers, Pranav Mundada, Basil M Smitham, Mattias Fitzpatrick, Zhaoqi Leng, Anjali Premkumar, Jacob Bryon, Sara Sussman, Guangming Cheng, et al. New material platform for superconducting transmon qubits with coherence times exceeding 0.3 milliseconds. *arXiv preprint arXiv:2003.00024*, 2020.

[31] Jaseung Ku, Vladimir Manucharyan, and Alexey Bezryadin. Superconducting nanowires as nonlinear inductive elements for qubits. *Physical Review B*, 82:134518, Oct 2010.

[32] Ansys hfss software, http://www.ansoft.com/products/hf/hfss/.

[33] F. B. Faramarzi, P. Mauskopf, S. Gordon, G. Che, P. Day, H. Mani, H. Surdi, S. Sypkens, P. Barry, E. Shirokoff, and R. B Thakur. An on-chip superconducting kinetic inductance fourier transform spectrometer for millimeter-wave astronomy. *Journal of Low Temperature Physics*, 199:867–874, May 2020.

[34] Hanhee Paik, D. I. Schuster, Lev S. Bishop, G. Kirchmair, G. Catelani, A. P. Sears, B. R. Johnson, M. J. Reagor, L. Frunzio, L. I. Glazman, S. M. Girvin, M. H. Devoret, and R. J. Schoelkopf. Observation of high coherence in josephson junction qubits measured in a three-dimensional circuit qed architecture. *Physical Review Letters*, 107:240501, Dec 2011.

[35] Sonnet software inc., https://www.sonnetsoftware.com/.